Canadian Mineralogist
Vol. 26, pp. 871-888 (1988)

TWO-STAGE HYDROTHERMAL FORMATION OF A LOWER PROTEROZOIC SEDIMENT-HOSTED MASSIVE SULFIDE DEPOSIT, NORTHERN LABRADOR TROUGH, QUEBEC

TIMOTHY J. BARRETT, ROBERT P. WARES AND JOSEPH S. FOX
Mineral Exploration Research Institute, Department of Geological Sciences, McGill University, Montreal, Quebec H3A 2A7

ABSTRACT

The Soucy #1 massive sulfide deposit in the northern Labrador Trough of Quebec represents one of the few known ancient sediment-hosted Cu–Zn deposits. Despite the regional deformation of the Lower Proterozoic host sequence, the deposit is very well preserved. The massive sulfide lens is up to 40 m thick and 400 m long, and averages $\approx$2% each of Cu and Zn (with $<$0.2% Pb). It consists of sub-spherical pyrite framboids in a fine-grained matrix of metal sulfides and ferruginous gangue minerals. The ore lens is conformably overlain by a more laterally extensive blanket of up to 50 m of laminated, aphanitic, base metal-poor sulfides, consisting of pyrite microspherules disseminated throughout a pyrrhotite - iron silicate matrix. The ore lens is hosted by silicate- and sulfide-facies iron-formation that occurs within a thick turbidite sequence. An alteration "pipe" beneath the lens is characterized by addition of iron, calcium, and most base metals, and removal of alkalis. Within the pipe, stilpnomelane, ferroan ankerite and sulfides were precipitated in veins and in adjacent sediments. A zone of more intense footwall alteration, $\approx$5m thick, occurs immediately beneath the massive sulfides. The two compositionally and texturally different types of sulfide bodies indicate that two fundamentally different hydrothermal discharge processes operated during sulfide deposition. The first was a high-intensity, high-temperature process that locally precipitated the Cu–Zn-rich sulfides of the main ore lens, probably within a sub-basin on a foundered continental margin. By contrast, the overlying laminated iron sulfides are interpreted as "fallout" material which precipitated from a saturated, non-circulating, euxinic bottom layer, following decline in the temperature and intensity of discharge. In the laminated sulfides, a gross trend of decreasing base and precious metal content with distance from the massive sulfide lens may reflect continued but feeble hydrothermal discharge in the areas of the ore lens. The chemical component of interbedded silicate- and sulfide-facies iron-formation and interlayered sulfide/clastic sediments occurring along strike from the laminated sulfides is interpreted as the result of "spillover" effects from the hydrothermally influenced bottom water layer located in the sub-basin. The favored paleotectonic setting for massive sulfide deposition is a collapsed continental margin formed during early rifting of a lower Proterozoic basin, prior to extrusion of a basaltic seafloor.

Keywords: massive sulfides, laminated sulfides, copper, zinc, hydrothermal, turbidites, alteration, iron-formation, Proterozoic, Labrador Trough, Quebec.

SOMMAIRE

Le gisement de sulfures massifs Soucy #1, situé dans le nord de la Fosse du Labrador au Québec, représente un exemple peu commun d'un gisement de Cu–Zn logé dans des sédiments. En dépit de la déformation régionale de la séquence encaissante d'âge Protérozoïque inférieur, le gisement est bien préservé. La lentille de sulfures massifs mesure 400 m de long et atteint 40 m d'épaisseur, et elle titre une moyenne de $\approx$2% en Cu et de $\approx$2% en Zn (avec $<$0.2% de Pb). Elle consiste en framboïdes quasi-sphériques de pyrite logés dans une matrice à grains fins composée de sulfures de métaux usuels et de gangue ferrugineuse. La lentille est recouverte par une couche concordante de sulfures qui est latéralement plus étendue et qui atteint 50 m d'épaisseur. Cette couche se compose de sulfures laminés et aphanitiques, pauvres en métaux usuels, consistant en microsphérules de pyrite disséminées dans une matrice de pyrrhotine et de sillicates de fer. Le gisement est logé dans une formation de fer composée d'unités interlitées des faciès silicatés et sulfurés; le tout est inclus dans une séquence épaisse de turbidites. Une pipe d'altération, sous-jacente à la lentille, est caractérisée par l'addition du fer, du calcium et de la plupart des métaux usuels, et par le lessivage des alcalis. À l'intérieur de la pipe, le stilpnomélane, l'ankérite ferrugineuse et les sulfures sont précipités dans des veines et dans les sédiments adjacents. Un horizon d'altération plus intense, d'une épaisseur de 5 m, se trouve immédiatement sous la lentille de sulfures massifs. Les deux amas de sulfures sont chimiquement et texturalement distincts et indiquent que deux processus hydrothermaux, étant fondamentalement différents, ont opéré lors de la mise en place des sulfures. Le premier était un phénomène de décharge de haute intensité et de haute température qui a précipité, localement, les sulfures riches en Cu–Zn de la lentille principale. Ce phénomène aurait eu lieu dans un bassin restreint situé sur une marge continentale effondrée. Par contraste avec la lentille principale, les sulfures de fer laminés sous-jacents sont interprétés comme étant le résultat d'une accumulation de matières retombées. Ils auraient été précipités d'une couche de fond saturée, stagnante et euxinique, suivant une baisse de la température et de l'intensité de la décharge hydrothermale. Dans l'unité de sulfures laminés, on observe une baisse des teneurs en métaux usuels en fonction de la distance approximative de la lentille de sulfures massifs, reflétant probablement un prolongement faible de la décharge hydrothermale près de la lentille principale. Les faciès silicatés et sulfurés de la formation de fer et des sédiments sulfurés/clastiques rubanés sont disposées latéralement par rapport aux sulfures laminés. Leur composante chimique est interprétée comme étant le résultat d'un déversement de la couche de fond saturée au delà des limites du bassin. Nous favorisons, comme milieu paléotectonique de la mise en place des sulfures massifs, une marge continentale effondrée qui s'est développée aux stades précoces de la formation d'un bassin d'âge Protérozoïque inférieur, avant l'extrusion de basaltes sur le fond marin.

Mots-clés: sulfures massifs, sulfures laminés, cuivre, zinc, turbidites, formation de fer, altération, hydrothermal, Protérozoïque, Fosse du Labrador, Québec.

INTRODUCTION

Sediment-hosted syngenetic Cu–Zn massive sulfide deposits are uncommon in the geological record and few have been described in detail, apart from those Phanerozoic deposits classified as "Besshi" type (Doi 1961, Klau & Large 1980, Fox 1984). Proterozoic sediment-hosted Cu–Zn deposits are even less common, although they do occur in geological settings that are similar to Phanerozoic ones, *i.e.*, rift-related volcano-sedimentary sequences.

The Soucy No. 1 sediment-hosted massive sulfide deposit is one of four such deposits in the northern Labrador Trough of Quebec (Wares *et al.* 1988). The deposit is 90 km west of Kuujjuaq, an Inuit community that serves as access to that region (Fig. 1). The deposit was explored intermittently between 1953 and 1980; drill-indicated ore reserves are estimated to be 5.44 Mt at 1.49% Cu, 1.80% Zn, 13.7 g/t Ag and 1.61 g/t Au.

The deposit is folded, intruded by gabbro sills, and partly recrystallized, but primary features are sufficiently well preserved to allow insights into the environment and mechanisms of formation of the sulfides. This paper describes the stratigraphic and geochemical characteristics of the deposit, and interprets them in terms of a composite model based on hydrothermal and sulfide depositional processes operating at modern oceanic spreading centers.

GENERAL STRATIGRAPHY AND TECTONIC SETTING OF THE LABRADOR TROUGH

The Labrador trough is a well-preserved, thrust-imbricate lower Proterozoic fold belt (2150–1850

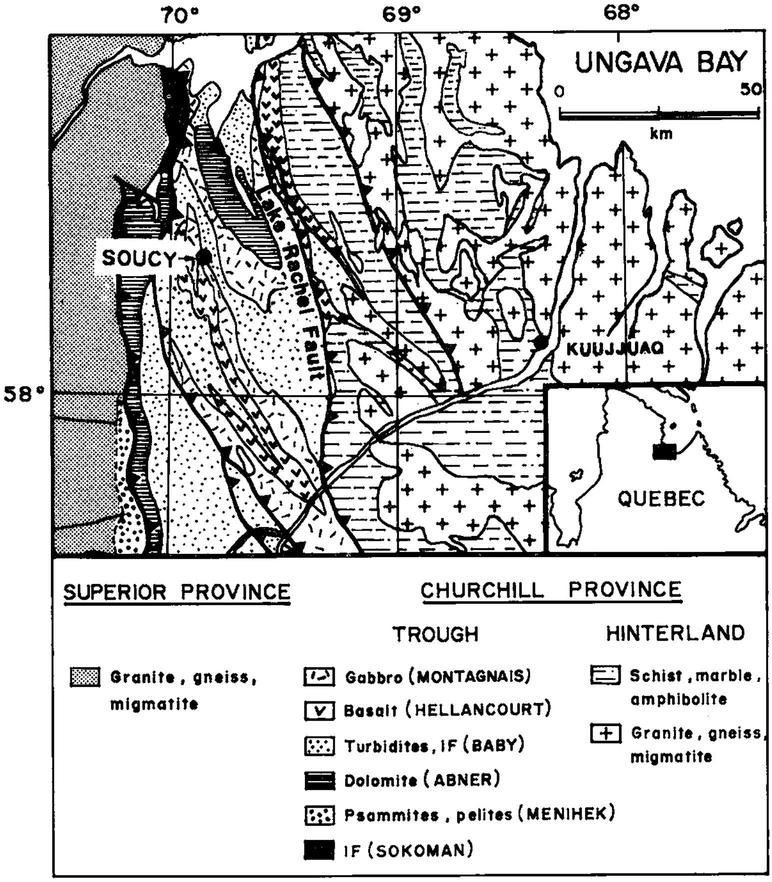

FIG. 1. Regional geology of the northern Labrador Trough and location of Soucy #1 massive sulfide deposit. Modified from map 2001, DV 85-09 (Ministère de l'Énergie et des Ressources du Québec).

Ma; Fryer 1972, Stockwell 1982) that stretches for 850 km from the Grenvillian metamorphic front to Ungava Bay. The trough represents the far-eastern extension of the Trans-Hudson Orogen, the deformed supracrustal sequences of which separate the Archean Superior and Churchill provinces.

The trough has been divided into three lithotectonic zones (Dimroth 1972, Dimroth & Dressler 1978, Dimroth 1981, Wardle & Bailey 1981): i) a western margin consisting mostly of autochthonous and parautochtonous platform sedimentary rocks resting unconformably on the Superior craton; ii) a central foreland fold-thrust belt, consisting of volcano-sedimentary sequences intruded by abundant gabbro sills. The foreland is of greenschist-facies metamorphic grade and exhibits westerly tectonic transport onto the craton; iii) a poorly defined eastern margin in the immediate hinterland consisting of amphibolite- and granulite-facies metasedimentary and metavolcanic rocks (Laporte Group), probably in part equivalent to rocks of the foreland belt, and of tectonized Archean rocks of the Churchill province.

The supracrustal sequence of the trough (Kaniapiskau Supergroup) consists of two distinct cycles of sedimentation and volcanism (Dimroth 1981, Wardle & Bailey 1981, LeGallais & Lavoie 1982, Clark & Thorpe submitted), primarily recognized in the Knob Lake Group. The upper Knob Lake Group (Fig. 2) comprises the platform sequence of the second cycle (Ferriman Subgroup), as well as overlying turbidites (Menihek Formation) and fluvial molasse (Chioak Formation).

The Gérido Group (unofficial name) constitutes the entirety of the foreland belt in the northern trough. The Gérido Group structurally overlies the upper Knob Lake Group, but is interpreted, for the most part, as a coeval, deeper water slope/rise sequence (Clark & Thorpe submitted). It is composed of the Abner dolomite at the base, the Baby Formation clastic-dominated sediments in the middle, and the Hellancourt basalts at the top. The whole sequence is intruded by gabbro sills of the Montagnais Group, which are in part comagmatic with the Hellancourt tholeiitic suite. The Baby Formation is divided into three members. The lower is heterogeneous, composed mostly of turbidites, and includes conglomerates, quartzites, wackes, siltstones and mudstones of variable thickness and proportion. The middle Baby is an iron-formation, ≈50-m thick, in the classic sense of the term (James 1954). It consists of oxide-, carbonate-, silicate- and sulfide-facies sediments distributed in an apparently heterogeneous manner (Clark 1987). The upper Baby consists mostly of rhythmically layered, thin-bedded distal turbidites and mudstones. Basalts are rare within the Baby Formation, and have not been mapped anywhere in the region of the Soucy deposit (Sauvé & Bergeron 1965, Wares *et al.* 1988). The Soucy deposit is located near the western margin of the foreland belt, and is hosted, along with other massive sulfide deposits in the region, within iron-formation of the middle Baby (Fig. 2).

The tectonic setting in which the Labrador trough supracrustal assemblage was deposited remains problematical. Dimroth (1972, 1981) and Dimroth & Dressler (1978) have postulated the development of a narrow, sediment-rich ensialic basin, generally floored by attenuated continental crust, which was filled by sequences of intercalated turbidites, tholeiites, and voluminous mafic subvolcanic sills. Hynes (1978), Wardle & Bailey (1981), and LeGallais & Lavoie (1982) also favor a rift setting, but emphasize that the tectonic setting of the rift is

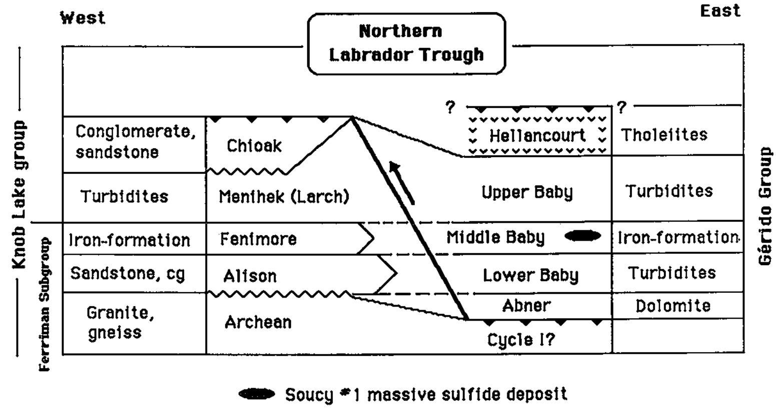

FIG. 2. Stratigraphic correlation chart for the Upper Knob Lake Group and the Gérido Group in the Northern Labrador Trough (cycle II sedimentary sequences). Location of the Soucy #1 massive sulfide deposit is shown.

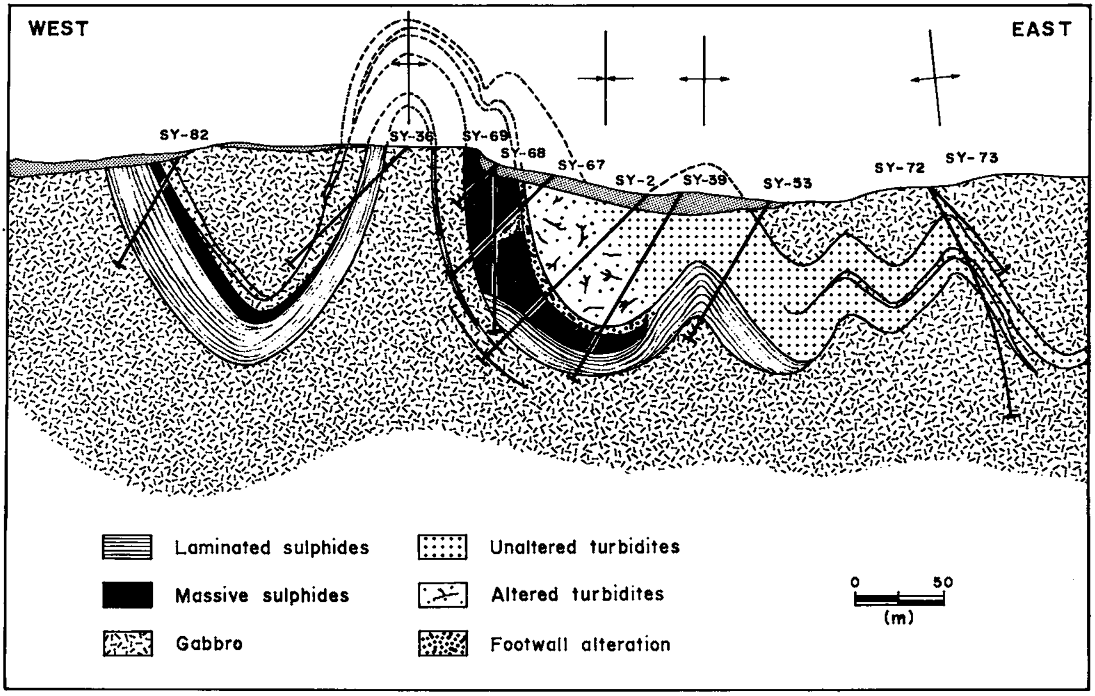

FIG. 3. Structural cross-section of the Soucy deposit, showing location of the diamond drillholes on which the structural interpretations of this section, and the stratigraphic column of Figure 4, are based.

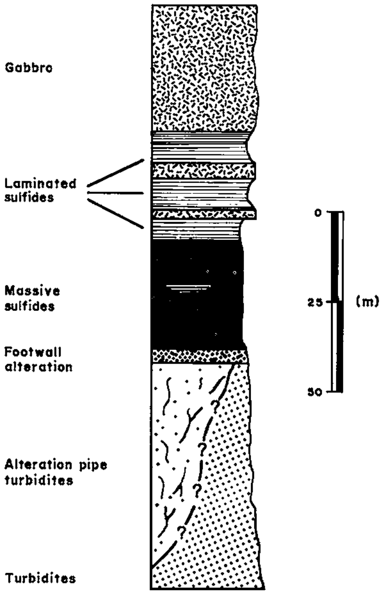

FIG. 4. Generalized stratigraphic column of the Soucy deposit at its thickest combined extent of massive and laminated sulfides (drillhole SY-2).

speculative because the supracrustal sequences represent only the vestiges of a collapsed, passive margin, and the nature of the high-grade metamorphic rocks of the eastern hinterland remains largely unknown. Although Hoffman (1987) recently postulated that deposition of cycle II sequences occurred in a migrating synorogenic foredeep, we consider an east-facing collapsed continental margin as a reasonable tectonic setting for accumulation of the Gérido Group, possibly during nascent seafloor spreading as is suggested by the presence of the voluminous tholeiitic volcanism.

GEOLOGY OF THE SOUCY DEPOSIT

The Soucy deposit lies on the east limb of the Lac Bourgault syncline (Fig. 1), an important structure that is traceable for at least 30 km. On surface the deposit outcrops as two subparallel NNW-striking zones of gossan. Drilling outlined two corresponding massive sulfide zones. The "A" zone, which is the main sulfide deposit, is overturned, lensoid, and extends along strike for at least 400 m. The "D" zone, 200 m to the west, is thinner, tabular and overturned, and traceable for at least 500 m along strike. These features are interpreted to represent an original semi-continuous lens of sulfide that has been affected by two coaxial deformations. The present morphology of the deposit is due to refolding, by tight upright structures, of the the limb of a west-verging isoclinal fold (Fig. 3). The abundance of lithologically homogeneous gabbro sills in the sequence surrounding the deposit does not permit a more detailed resolution of the local structure. Metamorphic grade is middle greenschist facies, which locally has caused destruction of finer primary sedimentological features in some lithologies. Nevertheless, the stratigraphy immediately above and below the main sulfide lens is well preserved.

As outcrop in the area of the deposit is extremely limited, the detailed stratigraphy (Fig. 4) was determined solely through examination of drill core. The main lithological units embracing the sulfide deposit are, from bottom to top: 1) unmineralized distal turbidites representing the regional host rock, referred to the lower Baby; 2) the "feeder pipe" alteration zone, of undetermined shape but occurring only below the massive sulfide lens; 3) a footwall alteration zone, 3 to 6 m thick, occurring immediately below the sulfide lens, and only as laterally extensive as the latter; 4) a lensoid polymetallic massive

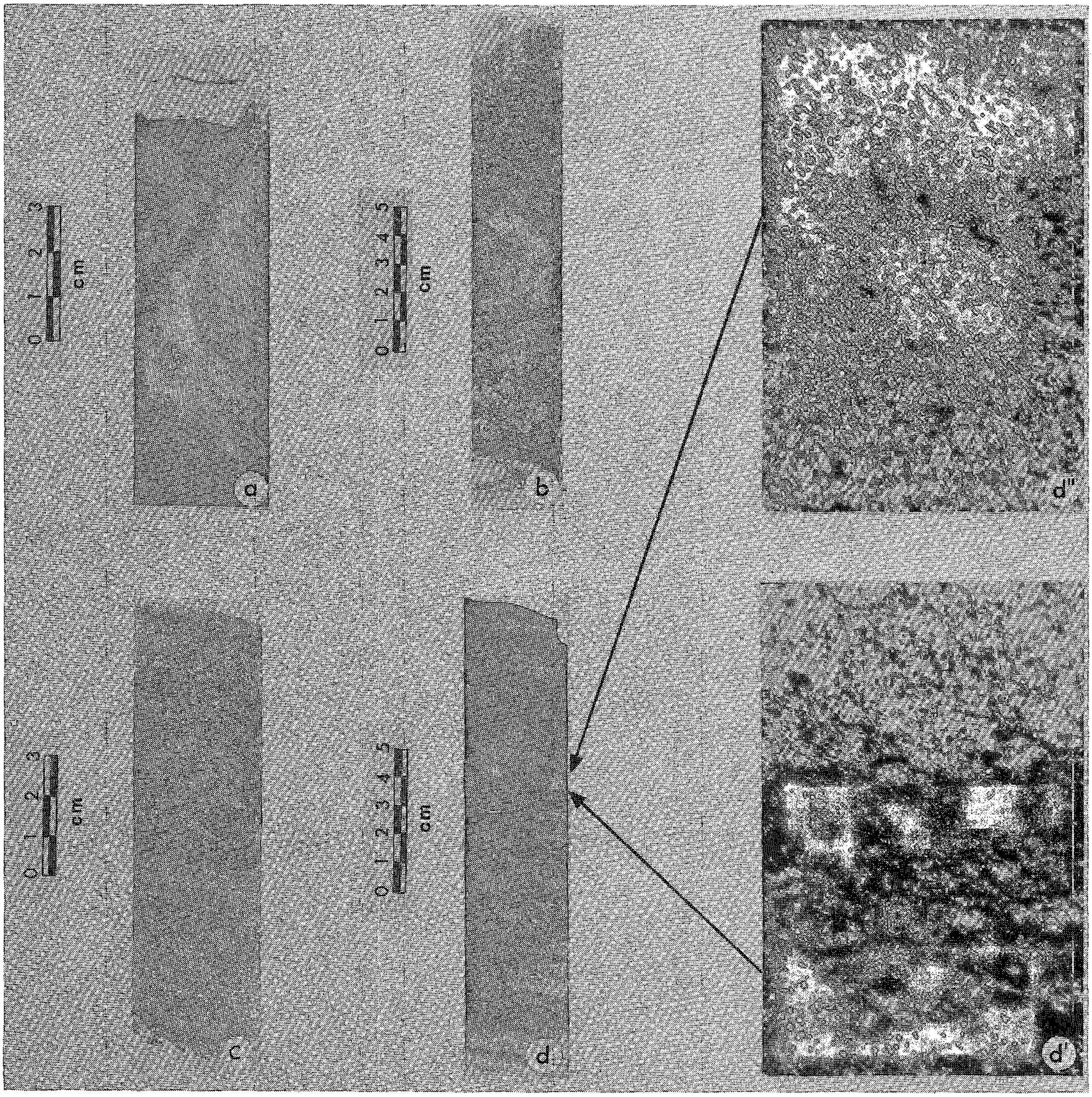

FIG. 5. a: Vein-proximal alteration in turbidites from alteration "pipe" below main sulfide lens; b: footwall alteration in turbidites; c: laminated sulfides; d: "banded clastic"/sulfide sediment consisting of thin silt beds and mm-scale silt laminations alternating with very fine-grained pyrite-rich sediment; d′ and d′′ are enlargements of the base and top, respectively, of a 5-mm-thick clastic silt bed (central interval not shown).

sulfide body up to 40 m thick; 5) laminated sulfides, also lensoid in shape and up to 50 m thick. This unit is laterally more widespread than the massive sulfides which it blankets. Its maximum extent is indeterminate, although it has been recognized in drillholes up to 200 m along strike from the main deposit. Units higher in the stratigraphy have been displaced by gabbro sills.

In addition to the massive sulfide to laminated sulfide transition at the perimeter of the massive sulfide lens, lateral lithofacies variants include the following units: 6) "banded" sediments consisting of

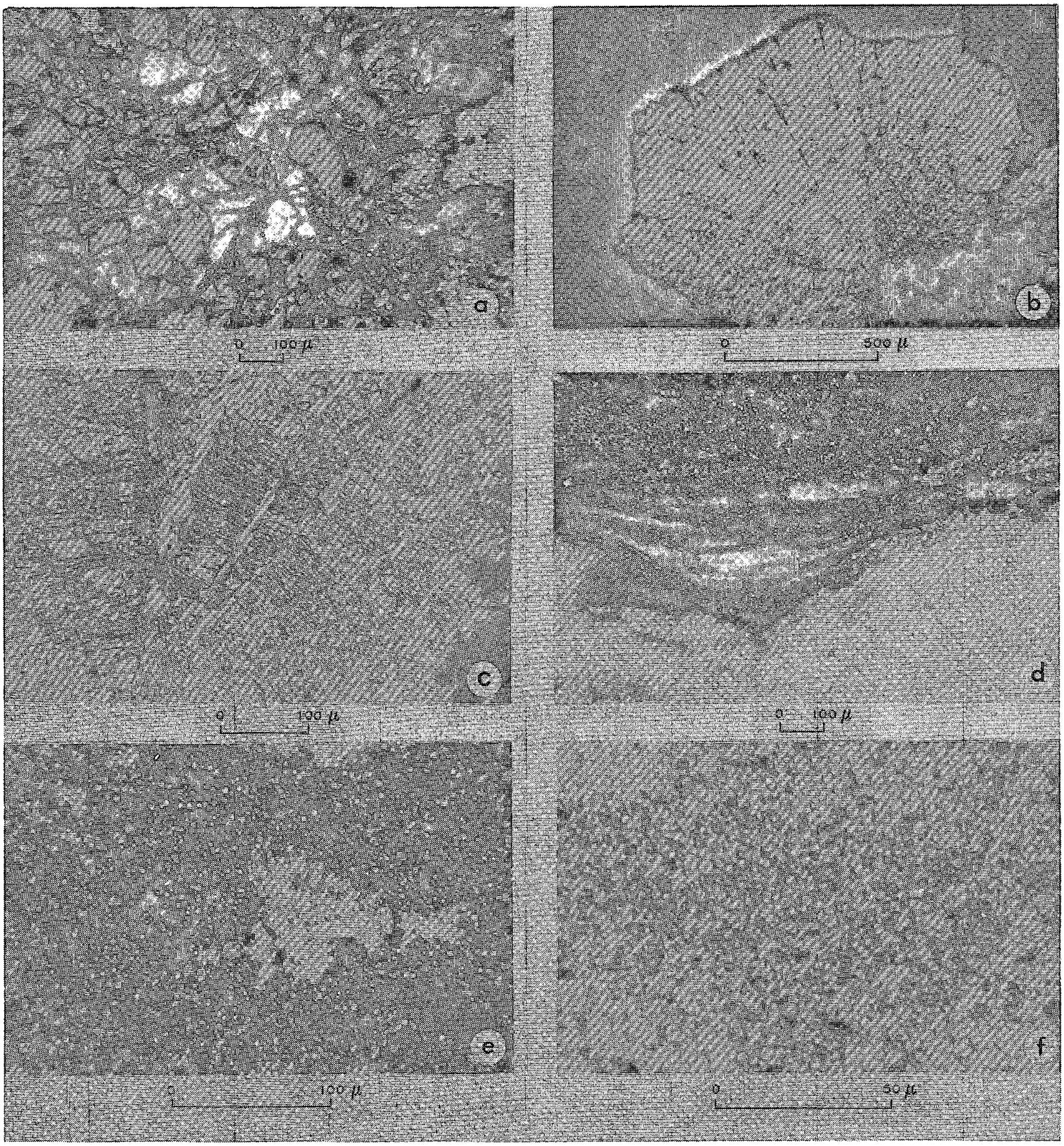

FIG. 6. Reflected-light photomicrographs of mineralogical textures and sedimentary features of sulfide-bearing lithologies. (a): medium-grained alteration assemblage in immediate footwall zone: stilpnomelane, ankerite, chlorite, alkali feldspar, magnetite and pyrrhotite are present; (b): pyrite "framboid" in massive sulfide; (c): replacement of pyrite framboid by pyrrhotite and chalcopyrite; (d): contact of laminated and massive sulfides; note sedimentary infilling textures; (e): close-up of laminated sulfides, showing pyrite microspherules and clot of pyrrhotite that replaced pyrite microparticles; (f): dense pyrite microparticle assemblage in pyrrhotite–chalcopyrite–iron silicate matrix; note chain-like arrays of particles.

thinly interbedded sulfidic–clastic layers; and 7) intercalated silicate-facies and sulfide-facies iron-formation.

Unit 1. Sediments underlying the ore lens are typically rhythmically layered, thin-bedded, light grey quartzofeldspathic siltstones, dark grey mudstones, and laminated argillites. Graded bedding and load casts are common, indicating that the beds are overturned. Mudstones may partly represent the upper fine-grained parts of siltstone turbidites. Argillites probably represent interturbidite sediments.

Unit 2. The "feeder pipe" alteration zone occurs within the sediments of Unit 1. The pipe is characteristically dark green and cut by irregular, mm-scale veins generally at high angles to bedding. These veins consist of coarse-grained ankerite, stilpnomelane, pyrrhotite and minor chalcopyrite. Intense wallrock alteration, comprising massive, fine-grained stilpnomelane and ankerite, extends for up to 1 cm from the veins and obliterates bedding (Fig. 5a). The ankerite also forms semi-continuous laminations that replace the coarser lower parts of the silt turbidites and obscures primary grading. Mudstones and argillites within this zone are pervasively enriched in alteration minerals.

The meandering, curving nature of the veins is a characteristic and important feature of this zone. We interpret these "wormlike" veins to be part of a feeder system; the style of veining suggests that the sediments were unconsolidated at the time of vein injection.

Unit 3. The footwall displays alteration over ≈5m immediately below the ore lens, but lacks the veins of the "pipe". Carbonate occurs as clots of 1–2 mm width that give the rock a distinctive spotted appearance (Fig. 5b). Primary sedimentary features have been almost obliterated and replaced by a medium- to fine-grained assemblage of stilpnomelane, ankerite, chlorite, grunerite, magnetite, alkali feldspar, mm-wide clots of pyrrhotite, and traces of disseminated chalcopyrite and sphalerite (Fig. 6a). The contact with the underlying feeder zone is gradual over 0.5 m.

Stilpnomelane is widespread in the Baby iron-formation of the Trough (Clark 1987), and is considered to be a low-temperature diagenetic or metamorphic phase of silicate iron-formation (Klein 1979). Stilpnomelane in the "pipe" and footwall zones may have been retrograded from a higher temperature hydrothermal assemblage. Ferruginous amphiboles, such as grunerite, are considered to be higher temperature products.

Unit 4. The contact between the footwall zone and the massive sulfide lens is sharp. The latter consists of sub-spherical pyrite framboids (1 to 3 cm wide) showing radiaxial internal structures (Fig. 6b) in a matrix of fine-grained, recrystallized, granoblastic pyrrhotite, chalcopyrite, sphalerite and traces of galena. Matrix gangue (10–15 vol. %) consists of ankerite, magnetite, and minor stilpnomelane and quartz. Pyrrhotite replaced pyrite framboids and magnetite, and is intergrown with carbonate and stilpnomelane. Chalcopyrite and sphalerite replaced the iron sulfides (Fig. 6c). The magnetite and pyritic framboids crystallized relatively early and may be either syngenetic or diagenetic.

Thin (<10 cm) lenticular beds of laminated sulfides also occur within the massive sulfide lens. These units are concordant with local bedding, and display small-scale sedimentary infilling textures at their lower contacts with massive sulfides (Fig. 6d). These beds are lithologically identical to the laminated sulfides of Unit 5.

Unit 5. The overlying laminated sulfides are a distinctive and important sediment lithofacies. Hand specimens are beige to chocolate-brown, aphanitic, and commonly display laminations <0.5 mm thick (Fig. 5c). Intervals up to a few cm in thickness that are devoid of lamination are also present. Because of their fine grain size, Unit 5 sulfides lack the metallic sheen of massive sulfides. The sediment consists of pyrite microspherules (5–10 μm diameter) disseminated throughout a coarser grained, recrystallized pyrrhotite – iron silicate – quartz – muscovite matrix (Fig. 6e). Irregular clots (0.1–5 mm wide) of pyrrhotite and chalcopyrite occur sporadically. The pyrite particles are either isolated or form short chain-like arrays (Fig. 6f). We interpret the pyrite particles to be a primary sedimentary feature; the sulfide matrix and clots, which are recrystallized, partly replace these particles.

The sub-mm-scale laminations are the result of alternating sulfide- and clastic-rich sediment. The clastic material is similar to that in the distal turbidites underlying and overlying the sulfide horizons (quartz–feldspar–mica). Silt turbidites up to 1 cm in thickness are locally present within the laminated sulfides, and display size grading, with increasing amounts of fine-grained sulfides towards the tops of beds. Aphanitic sulfide sediments lacking lamination contain scattered patches of quartz silt and coarser muscovite flakes.

Unit 6. "Banded" sediments consist of regular alternations of mm-scale sulfide-rich layers and silty turbidite layers (Fig. 5d). The laminated sulfides of Unit 5 pass laterally and locally upward into "banded" sediments through gradual increase in the number and thickness of the clastic intercalations. Microscopic textures in the thin sulfide-rich layers of the "banded" sediments are similar to those in the laminated sulfide unit. The silty turbidites, which are generally less than 1 cm thick, commonly grade from a light-colored lower siltstone to an overlying dark silty mudstone which represents the top of the turbidite. This sequence is followed either by: i) a sulfide-rich layer ≈5 mm thick; ii) a very dark mudstone ≈ 5 mm thick; or iii) a compound layer containing 2 to 3 sulfide-rich and mudstone-rich laminations, each 1–2 mm thick.

Unit 7. The laterally associated silicate-facies iron-formation generally consists of dark green to brownish mudstones containing abundant stilpnomelane and grunerite, carbonate, minor disseminated iron sulfides, and scattered quartz and feldspar. The iron-bearing minerals also occur as thin stringers subparallel to bedding, forming very dark layers ≈ 5 mm thick. Thin, light-colored interbeds are common although of variable proportion; they are rich in muscovite and coarser quartz and sulfides, and contain minor plagioclase. The interbeds resemble the silty beds of the turbidites, but are coarser grained due to strong recrystallization.

Laminated sulfide-facies iron-formation interbedded on the outcrop scale with the silicate-facies iron-formation is perhaps more appropriately termed pyritic, graphitic slate. However, we maintain this term as it is conventionally employed in Labrador Trough mapping.

GEOCHEMISTRY

Thirty-two samples of various lithofacies have been analyzed for major and trace elements, and an additional 59 samples for trace elements and iron only. The data are given in Tables 1 and 2, respectively.

Massive and laminated sulfides. Massive sulfides analyzed in this study (17 samples) have an average composition of 1.28% Cu, 2.38% Zn and 0.19% Pb, with 22 g/t Ag and 0.8 g/t Au. Factor analysis (Table 3) indicates that the dominant components in the massive sulfides are: Zn–Cu–Pb–Ag–Au (44% of the variance), Fe–Co–Au (27%), and Cu–Ni–Au (29%). The first two components represent base-metal-dominated and iron-sulfide-

TABLE 1. CHEMICAL COMPOSITION OF MAIN LITHOLOGICAL UNITS AT THE SOUCY #1 MASSIVE SULFIDE DEPOSIT, LABRADOR TROUGH

Sample	SiO_2 %	TiO_2 %	Al_2O_3 %	Fe_2O_3 %	MnO %	MgO %	CaO %	Na_2O %	K_2O %	P_2O_5 %	LOI %	Total %	Cu ppm	Zn ppm	Pb ppm	Ni ppm	Co ppm	V ppm	Ba ppm	Ag ppm	Au ppb	ΣBM ppm
Silicate iron formation																						
RW-2697-86	59.3	0.08	2.55	30.9	0.84	2.41	2.07	1.04	0.06	0.07	0.01	99.4	10	13	14	10	161	22	51	0.1	1	37
RW-3149A-86	48.9	0.25	7.43	27.9	0.19	3.09	0.50	0.01	0.93	0.28	11.1	100.6	185	92	21	63	166	78	159	0.3	4	298
RW-3150C-86	66.8	0.09	3.11	14.9	0.50	3.43	5.88	0.08	0.64	0.04	4.80	100.3	64	11	5	10	63	10	144	0.1	2	80
RW-3150G-86	66.4	0.12	3.43	20.2	0.27	3.30	0.94	0.03	1.26	0.10	3.85	100.0	20	38	5	10	96	26	234	0.1	1	63
RW-1196A-86	53.3	0.20	7.12	21.9	0.51	8.30	5.50	0.01	0.05	0.15	2.61	99.6	31	82	5	10	124	46	9	0.1	2	118
SY-12 (235-236)	38.3	1.09	12.0	26.8	0.05	1.88	1.63	1.29	2.50	0.15	14.0	99.6	113	432	32	60	172	152	280	0.5	6	577
SY-88-98	49.7	0.56	12.4	24.1	0.05	2.01	0.11	0.01	3.42	0.05	7.90	100.2	26	10	20	86	118	223	185	0.5	6	56
Average	**54.7**	**0.34**	**6.86**	**23.8**	**0.34**	**3.49**	**2.38**	**0.35**	**1.27**	**0.12**	**6.32**	**100.0**	**64**	**97**	**15**	**36**	**129**	**80**	**152**	**0.2**	**3**	**176**
"Banded" sediment																						
RW3206A-86	44.8	0.71	11.2	27.4	0.06	2.99	1.05	0.95	2.98	0.09	8.74	101.0	780	22	5	126	99	269	545	0.2	1	807
Laminated sulfides*																						
SY-1-313 P	23.3	0.44	5.94	49.9	0.05	4.19	0.56	1.03	0.37	0.10	14.9	100.7	2076	950	79	96	527	101	65	3.6	63	3110
SY-2 (330-331) P	13.5	0.44	5.54	56.4	0.09	3.88	0.39	0.28	0.54	0.08	19.2	100.4	3315	2645	262	136	394	117	64	8.2	2	6220
SY-9 (461-462) D	23.1	0.31	5.88	46.1	0.02	0.61	0.73	0.87	0.95	0.06	21.3	99.9	411	250	114	48	281	64	184	1.1	30	775
SY-12 (242-243) D	27.3	0.54	7.96	41.1	0.04	1.53	2.38	1.87	0.65	0.08	16.7	100.2	291	559	53	81	254	129	167	0.8	17	903
SY-37-363 P	15.0	0.29	4.31	55.4	0.05	2.18	0.20	0.56	0.72	0.04	21.4	100.2	9800	15200	1352	263	463	72	94	14.8	320	26400
SY-82 (169-170) D	25.9	0.52	7.48	41.1	0.02	1.40	0.07	0.01	1.52	0.04	22.7	100.8	40	595	36	85	244	106	163	0.5	1	671
RW3206E-86 D	38.8	0.68	10.3	33.4	0.03	1.94	0.73	3.79	0.67	0.04	9.61	100.0	105	124	5	125	111	171	101	0.8	2	234
Average	**23.8**	**0.46**	**6.77**	**46.2**	**0.04**	**2.25**	**0.72**	**1.20**	**0.77**	**0.06**	**18.0**	**100.3**	**2201**	**2900**	**272**	**119**	**325**	**109**	**120**	**4.3**	**62**	**5470**
Footwall alteration																						
SY-2-269	42.5	0.61	8.70	35.7	0.09	1.44	4.30	2.01	2.01	0.14	2.98	100.4	1004	212	33	135	393	159	54	0.9	25	1250
SY-5-(87-88)	30.3	0.52	8.18	48.3	0.09	6.90	2.41	1.81	1.09	0.11	5.73	100.2	3327	243	27	73	417	96	76	1.8	30	3600
Average	**36.4**	**0.57**	**8.44**	**42.0**	**0.09**	**4.17**	**3.36**	**1.91**	**1.55**	**0.13**	**4.36**	**100.3**	**2170**	**228**	**30**	**104**	**405**	**128**	**65**	**1.4**	**28**	**2420**
Altered "pipe" turbidites																						
SY-2-97	51.4	0.59	9.46	22.7	0.15	3.99	5.56	0.01	0.04	0.07	4.90	98.8	134	141	5	184	150	399	18	0.2	4	280
SY-2-107	49.8	0.27	4.57	17.7	0.22	2.57	12.4	0.10	0.56	0.06	10.9	99.2	16	123	5	62	129	129	37	0.1	3	144
SY-2-125	44.2	0.96	8.80	26.4	0.21	3.34	8.49	0.01	0.25	0.14	4.89	97.7	99	156	7	81	182	182	66	0.2	5	262
SY-2-227	64.5	0.66	10.1	15.1	0.07	4.70	0.31	0.01	0.34	0.10	4.03	99.9	98	158	5	41	91	91	42	0.1	2	261
SY-2-253	50.7	0.76	12.3	23.4	0.14	4.34	2.78	0.01	0.47	0.12	4.30	99.3	125	74	7	84	134	134	98	0.3	6	206
SY-2-256	41.2	0.63	12.6	36.4	0.14	3.03	0.88	0.11	0.07	0.08	5.45	100.7	250	98	11	50	238	238	65	0.4	19	359
Average	**50.3**	**0.65**	**9.64**	**23.6**	**0.16**	**3.66**	**5.07**	**0.04**	**0.29**	**0.10**	**5.75**	**99.3**	**120**	**125**	**7**	**84**	**154**	**196**	**54**	**0.2**	**7**	**252**
Unaltered turbidites																						
SY-2-58	49.8	0.66	13.9	13.8	0.15	6.16	6.37	0.03	1.51	0.06	7.49	100.0	29	118	5	98	78	176	252	0.2	1	152
SY-9-328	62.5	0.52	13.5	10.7	0.04	2.63	1.93	3.65	1.79	0.06	3.24	100.6	66	236	10	35	45	129	224	0.1	1	312
SY-11(225-226)	53.6	1.03	14.4	16.2	0.06	3.51	1.13	4.62	0.54	0.17	4.55	99.8	182	35	6	59	91	130	116	0.1	1	223
SY-21-135	58.9	0.82	15.9	12.6	0.06	2.77	0.46	0.04	4.11	0.07	4.52	100.2	76	393	7	45	63	318	302	0.3	4	476
SY-37-281	67.4	0.63	11.4	13.8	0.07	2.14	0.13	0.01	1.61	0.09	3.24	100.4	95	138	5	33	72	158	261	0.1	1	238
SY-90-118	62.5	0.64	18.7	6.75	0.05	2.93	0.45	0.58	4.28	0.06	3.48	100.4	68	79	5	61	26	203	393	0.1	1	152
RW-3151-86	64.2	0.61	16.5	8.09	0.44	1.60	0.13	1.50	4.78	0.07	2.63	100.5	34	51	6	27	45	54	1500	0.1	1	91
RW-3272E-86	55.8	0.33	10.2	18.4	0.41	4.46	0.98	0.60	0.93	0.07	7.83	100.0	93	83	6	40	105	69	332	0.1	2	182
RW-3295A-86	57.0	1.00	18.8	12.5	0.09	2.50	0.41	1.59	3.66	0.11	2.98	100.6	27	89	7	34	64	90	448	0.1	1	123
Average	**59.1**	**0.69**	**14.8**	**12.5**	**0.15**	**3.19**	**1.33**	**1.40**	**2.58**	**0.08**	**4.44**	**100.3**	**74**	**136**	**6**	**48**	**65**	**147**	**425**	**0.1**	**1**	**217**

* P = proximal, D = distal

Note: ΣBM = Cu + Zn + Pb.

dominated groups, respectively, whereas the third component may reflect a Ni-bearing sulfide.

The laminated sulfides have an iron content comparable to that of the massive sulfides (≈ 26 *versus* $\approx 30\%$, respectively), but contain only 0.32% Zn and 0.15% Cu, and much lower Au and Ag contents. When the laminated sulfides are subdivided into "proximal" facies (*i.e.*, overlying the ore lens) and "distal" facies (*i.e.*, lateral to the ore lens), concentrations of Cu, Zn, Pb, Ag and Au all show a further significant decrease over distances of up to a few hundred meters from the massive sulfides (*e.g.*, Fig. 7). Thus, there are primary dispersion patterns for these metals within the laminated sulfide horizon. Factor analysis of major-element data indicates that the variance in the laminated sulfides is due to three components (dominant elements in brackets), interpreted as: 1) detrital quartz–plagioclase–rutile (Si–Ti–Al–Na: 33% of variance); 2) hydrothermal sulfides-oxides (Fe–Mn: 32%); and 3) an assemblage reflecting hydrothermal silicates–carbonates (Mg–Ca–Mn–Fe–P: 25%). The trace-element variance in these sulfides, based on a larger sample set, is controlled by three factors (Table 3). These factors are interpreted as: 1) base metal sulfides and associated precious metals (Cu–Zn–Pb–Co–Ag–Au: 62%); 2) iron sulfides (Fe–Co–Pb: 21%); and 3) possible manganese oxide scavenging (Ni–Pb–Mn–Ag: 18%).

Figures 7c and 7d display geochemical trends for Au, Ag, and base metals in the four vertically continuous units: host turbidites, "pipe" and footwall alteration zones, massive sulfides, and laminated sulfides. Although each of the lithological units overlaps chemically, there is a general increase in precious and base metal content from turbidites to footwall alteration to laminated sulfides to massive sulfides.

Footwall alteration. Figures 8a and 8b show the average major- and trace-element compositions of unaltered and altered "pipe" turbidites. Assuming constant-volume alteration, which is suggested by apparently unmodified sedimentary textures such as smooth gradation and load casts in the turbidites, the alteration "pipe" is strongly depleted in K, Na and Ba, and slightly depleted in Si and Al relative to unaltered turbidites. Altered turbidites are enriched in Fe and Ca, as well as in most trace metals. Mg, Mn, Ti and P were apparently immobile during footwall alteration.

The most pronounced major-element compositional changes during alteration are plotted in Figures 8c and 8d: enrichment in Fe (sulfides, iron silicates) and in Ca (ankerite) accompanies a depletion in alkalis (leaching of the feldspathic component). The weakly correlated regression line included in Figure 8c indicates that there is variation in $Fe_2O_3/Na_2O + K_2O$ in the unaltered turbidites, caused by the relative proportions of detrital ferromagnesian minerals and feldspar. The altered turbidites depart from this trend. (The enrichment in Ca in one unaltered turbidite in Figure 8d is due to 20% diagenetic calcite micronodules.)

TABLE 2. TRACE ELEMENT AND Fe CONTENT OF MAIN LITHOLOGICAL UNITS AT THE SOUCY #1 MASSIVE SULFIDE DEPOSIT, LABRADOR TROUGH

Sample	Cu ppm	Zn ppm	Pb ppm	Ni ppm	Co ppm	Mn ppm	Fe %	Ag ppm	Au ppb	ΣBM ppm
					"Banded" sediments					
SY-33-196	148	48	11	75	38	501	16.6	1.0	1	207
SY-40-360	197	127	25	70	50	1130	20.8	0.4	1	349
SY-81-213	137	42	20	64	30	675	16.8	0.4	11	199
RW-0067D-86	265	24	11	33	52	485	7.1	0.1	5	300
RW-0067E-86	97	26	9	42	24	220	3.6	0.1	3	132
RW-0070A-86	694	35	9	146	75	320	14.3	0.4	5	738
RW-0072C-86	262	225	12	184	46	520	20.9	0.3	11	499
Average	**257**	**75**	**14**	**88**	**45**	**550**	**14.3**	**0.4**	**5**	**346**
					Silicate iron-formation					
SY-9(240-241)	258	234	60	165	71	399	24.3	0.7	6	552
SY-9(348-349)	122	952	33	109	45	426	16.8	0.3	1	1110
SY-11(225-226)	182	35	6	59	91	600	11.4	0.1	1	223
SY-12(207-208)	82	20	18	68	51	376	11.3	0.1	1	120
RW-0106A-86	347	69	39	83	100	290	21.6	0.1	1	455
RW-3171-86	968	103	15	150	84	510	21.9	0.2	1	1090
RW-3206H-86	138	68	28	109	104	265	24.8	0.2	1	234
Average	**300**	**212**	**28**	**106**	**78**	**409**	**18.9**	**0.2**	**2**	**541**
					Sulfide iron-formation					
SY-40-287	63	22	29	104	52	375	20.9	0.3	4	114
SY-90-220	498	70	13	169	123	750	24.3	0.2	2	581
SY-90-250	292	57	9	107	49	900	13.7	0.1	1	358
RW-0076H-86	108	192	33	14	25	75	14.4	0.9	7	333
RW-0104-86	377	246	123	56	149	65	20.6	0.1	1	746
RW-1067A-86	9	9	22	5	5	199	2.6	0.1	5	40
RW-1179B-86	380	851	15	153	113	1140	29.9	0.2	1	1250
RW-1213D-86	240	50	37	106	89	55	19.2	0.2	5	327
RW-2620A-86	411	553	23	142	46	70	21.5	0.2	1	987
RW-3120-86	7	13	20	5	5	130	2.8	0.5	1	40
RW-3196C-86	570	38	6	64	57	65	11.9	0.2	1	614
Average	**269**	**191**	**30**	**84**	**65**	**348**	**16.5**	**0.3**	**3**	**490**
					Laminated sulfides*					
SY-1-329 P	8510	5920	66	79	194	547	22.4	1.7	82	14500
SY-4(6-17) P	4360	21500	352	85	589	301	27.0	8.9	750	26200
SY-4(113-114) P	2900	1850	215	122	345	475	33.5	5.0	310	4970
SY-37-376 P	1500	2700	41	177	11	3650	17.3	2.2	19	4240
SY-37-385 P	346	3150	418	147	131	475	22.4	4.6	199	391
SY-40-302 P	457	100	55	228	66	424	30.2	1.0	4	612
SY-82-135 D	111	999	105	197	121	499	22.9	0.6	31	1220
SY-82-190 D	97	799	105	226	135	599	26.7	0.3	25	1000
RW-0076N-86 D	75	22	67	89	116	50	21.2	0.8	22	164
RW-00760-86 D	736	254	43	168	95	55	27.2	0.1	10	1030
RW-0115-86 P	632	3650	400	87	43	475	27.4	2.8	3	4680
RW-3206C-86 D	82	535	82	159	170	125	23.9	0.7	1	699
RW-3206D-86 D	65	27	14	176	175	130	31.1	0.1	4	106
Average	**1530**	**3190**	**151**	**149**	**169**	**600**	**25.6**	**2.2**	**112**	**4870**
					Massive sulfides					
SY-1(289-290)	11500	2300	441	26	1080	1850	33.3	12.3	780	14300
SY-2(304-305)	10000	15500	1530	19	217	6930	28.8	15.8	370	27000
SY-3(210-212)	7360	1890	287	10	1080	1040	36.3	12.1	850	9530
SY-3(227-228)	6310	34000	460	14	1110	3580	30.4	12.2	770	40800
SY-3(260-262)	8650	200	1090	40	665	375	37.3	12.3	198	9950
SY-5(105-108)	35400	25900	357	19	1390	1100	33.9	45.2	1910	61700
SY-5(121-123)	6410	61100	7240	29	500	1780	27.2	48.7	540	74800
SY-82(81-82)	7000	51000	684	27	114	1320	27.7	16.1	150	58700
RW-0113A-86	6860	6010	800	8	268	4210	29.3	8.7	310	13700
RW-0113B-86	4450	10300	1250	8	211	3030	25.9	8.2	395	16000
RW-0114A-86	3250	3350	1690	14	660	3980	33.2	12.2	485	8290
RW-0116A-86	6460	22000	3810	7	325	5760	29.6	16.9	315	32300
RW-0116B-86	2600	55600	9400	8	516	3080	25.3	29.2	325	67600
RW-0116C-86	13000	7920	1270	11	466	7290	29.5	24.9	865	22200
RW-0117A-86	43500	66500	209	110	498	190	23.4	48.0	1390	110200
RW-0117C-86	6390	1750	280	11	88	619	30.7	8.8	1620	8420
RW-0117D-86	37700	38500	225	90	344	245	26.7	44.2	1650	76400
Average	**12800**	**23800**	**1830**	**27**	**561**	**2730**	**29.9**	**22.1**	**760**	**38300**
					Footwall alteration					
SY-2(258-259)	2100	42	51	152	464	1525	18.8	2.2	13	2193
SY-3(92-93)	752	173	45	108	173	1829	23.9	0.7	20	970
Average	**1430**	**108**	**48**	**130**	**319**	**1680**	**21.4**	**1.5**	**16.5**	**1580**

* P = proximal, D = distal

Note: ΣBM = Cu + Zn + Pb.

Averages and ΣBM are rounded off to 3 significant figures

The immediate footwall alteration zone generally shows similar, if not more advanced, chemical alteration trends (Si, Al depletion; Fe enrichment). An important difference is that the alkalis are enriched (in the form of alkali feldspar) rather than depleted

TABLE 3. FACTOR ANALYSIS FOR TRACE ELEMENTS IN SOME LITHOLOGICAL UNITS, SOUCY #1 DEPOSIT, NORTHERN LABRADOR TROUGH

	Massive sulfides			Laminated sulfides		
Factor	1	2	3	1	2	3
Variance	.435	.274	.292	.616	.201	.193
Cu	.566	.307	.688	.793	.090	.259
Zn	.928	-.214	-.014	.962	-.048	-.002
Pb	.527	-.253	-.695	.647	.326	.505
Ni	.158	-.455	.767	-.021	-.098	.889
Co	.109	.831	.007	.735	.465	-.150
Mn	-.127	.069	-.648	.106	-.692	.334
Fe	-.347	.833	-.200	.239	.861	.256
Ag	.914	.224	.190	.848	.281	.353
Au	.360	.601	.522	.883	.007	-.200
Cu+Zn+Pb	.958	-.053	.214	.973	.010	.109

	Altered turbidites			Silicate iron formation		
Factor	1	2	3	1	2	3
Variance	.505	.349	.146	.360	.373	.267
Cu	.872	.413	-.090	-.204	.836	-.089
Zn	-.181	.956	-.224	.147	-.068	.957
Pb	.767	.051	.262	.484	.813	.291
Ni	-.013	-.128	.980	.420	.649	.384
Co	.879	.262	.217	.561	-.257	-.452
Mn	-.480	-.726	-.413	.244	-.798	-.092
Fe	.499	.837	-.106	.588	.771	.099
Ag	.968	-.083	.111	.956	.143	.138
Au	.578	.772	.004	.966	.065	.210
Cu+Zn+Pb	.855	.453	-.095	.102	.230	.908

*Principal component analysis. Transformation method: Orthotran-Varimax. Only three most important factors given.

as they are in the alteration "pipe". This suggests that the alkali-leaching process effective in the pipe was interrupted, and in fact reversed, near the sediment–seawater interface prior to or during sulfide deposition.

Silicate iron-formation. Relative to laminated sulfides, silicate iron-formation (SIF) is enriched in Si, Mn, Mg and Ca, reflecting the abundance of ferromagnesian and carbonate minerals. SIF is depleted in Fe and all trace metals with the exception of V. Factor analysis of major-element data indicates that SIF is dominated by a detrital component (K–Al–Ti: 42%), together with hydrothermal (Fe: 17%) and secondary detrital (Na–Ti: 15%) components. Si is a fairly strong negative factor in all three components, indicating that free silica has a diluting effect on the three components.

Figure 9a shows a negative correlation between Fe and Si in laminated sulfides and unaltered turbidites. This indicates that the hydrothermal supply of Fe (as sulfide) acted as a diluent to Si supplied by clastic material in the laminated sulfides. The fact that silica decreases with increasing iron content rules out any significant hydrothermal contribution of silica in the laminated sulfides. Several SIF samples plot between the turbidites and laminated sulfides, suggesting that SIF contains both detrital silica and hydrothermal iron. The majority of SIF samples does not show an increase in Al with Si (Fig. 9b), as would be expected if the Al were associated with clastic silicates. The low Al values are consistent with the abundance of stilpnomelane and grunerite in the samples.

DISCUSSION

The Cu–Zn-rich composition of the Soucy massive sulfides is unusual for exhalative sediment-hosted massive sulfides, which tend to be Zn–Pb-rich (Gustafson & Williams 1981). The composition is in fact more typical of massive sulfides contained in bimodal volcanic sequences (Franklin *et al.* 1981). Sediment-hosted Cu–Zn massive sulfide deposits comparable to the Soucy sulfides occur in the Sambagawa Schist Group, interpreted as a mixed metamorphosed volcanic-sedimentary sequence (Kanehira & Tatsumi 1970). These deposits, known as Besshi-type, typically have Cu:Zn ratios of ≈3 and are enriched in Co (≈1000 ppm). They are usually tabular or lenticular in shape and they apparently lack stringer alteration zones. Also ascribed to the Besshi type are other Cu–Zn sulfide deposits, with variable Cu–Zn ratios, which are hosted mainly by fine-grained terrigenous sediments (Fox 1984, 1988). These include deposits at Windy Craggy, Goldstream and Anyox in British Columbia, in the Blue Ridge belt of southeastern U.S.A. (Ducktown deposit: Stephens *et al.* 1984), in the Trondheim region of the Norwegian Caledonides (Nilsen 1978, Frietsch *et al.* 1979), and at Green Mountain, California (Mattinen & Bennett 1986). The Soucy deposit differs from these occurrences in having a footwall alteration zone, lower cobalt contents in the massive sulfides, a thick laminated sulfide blanket above the massive sulfides, and a regional setting within iron-formation (although metamorphosed iron-formation is associated with Cu–Zn deposits of the Kvikne district in the Norwegian Caledonides). The absence of some of these features in Besshi-type deposits may simply be a function of their higher metamorphic grade. Many of these deposits are thought to have formed in a tectonic setting analogous to that postulated for Soucy, *e.g.*, the Caledonian deposits are located on the outer Baltoscandinavian shelf wedge (Gee 1975), and Ducktown in a failed continental rift related to the opening of the Iapetus (Feiss & Hauck 1980).

In modern oceans, only the sulfide-facies muds in the Atlantis II Deep of the Red Sea are significantly enriched in Zn and Cu (≈10% Zn and 2% Cu on a salt-free basis: Bäcker 1976), but these overlie young oceanic tholeiites flanked by thick evaporite sequences. The bulk composition of all facies of metalliferous muds in this Deep is ≈3.4% Zn and ≈1.3% Cu (Bignell *et al.* 1976).

The laminated sulfides

This unit extends at least a few hundred meters

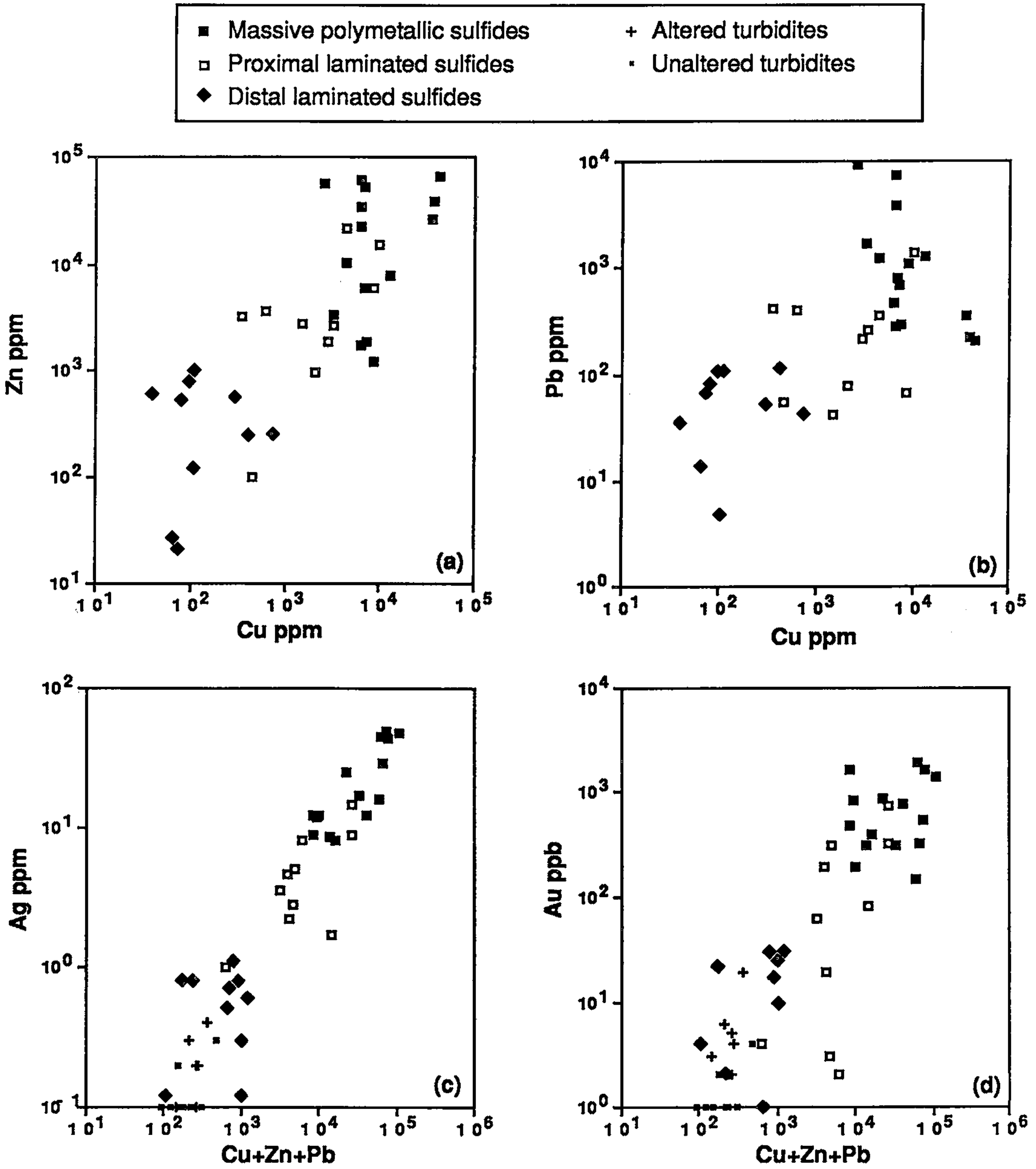

FIG. 7. Base and precious metal variations in massive and laminated sulfides at the Soucy deposit. Laminated sulfides are divided into "proximal" and "distal" locations relative to the ore lens. (a): Zn *versus* Cu; (b); Pb *versus* Cu; (c): Ag *versus* Cu + Zn + Pb; (d) Au *versus* Cu + Zn + Pb. In c and d, unaltered and altered turbidites are also shown.

beyond the limit of massive sulfide deposition. The fine lamination could reflect pulses of hydrothermal activity superimposed on a steady background accumulation of fine-grained clastic sediment. Lamination of apparently hydrothermal origin on a mm- to sub-mm scale has been documented in modern sulfides (Koski *et al.* 1984, Graham *et al.* 1988), and postulated for an Archean pyritic sulfide deposit (Fralick *et al.* accepted). On the other hand, episodic distal turbidites or annual clastic varving could interrupt more-or-less steady hydrothermal fallout. Sulfides with detrital microlaminations occur in the

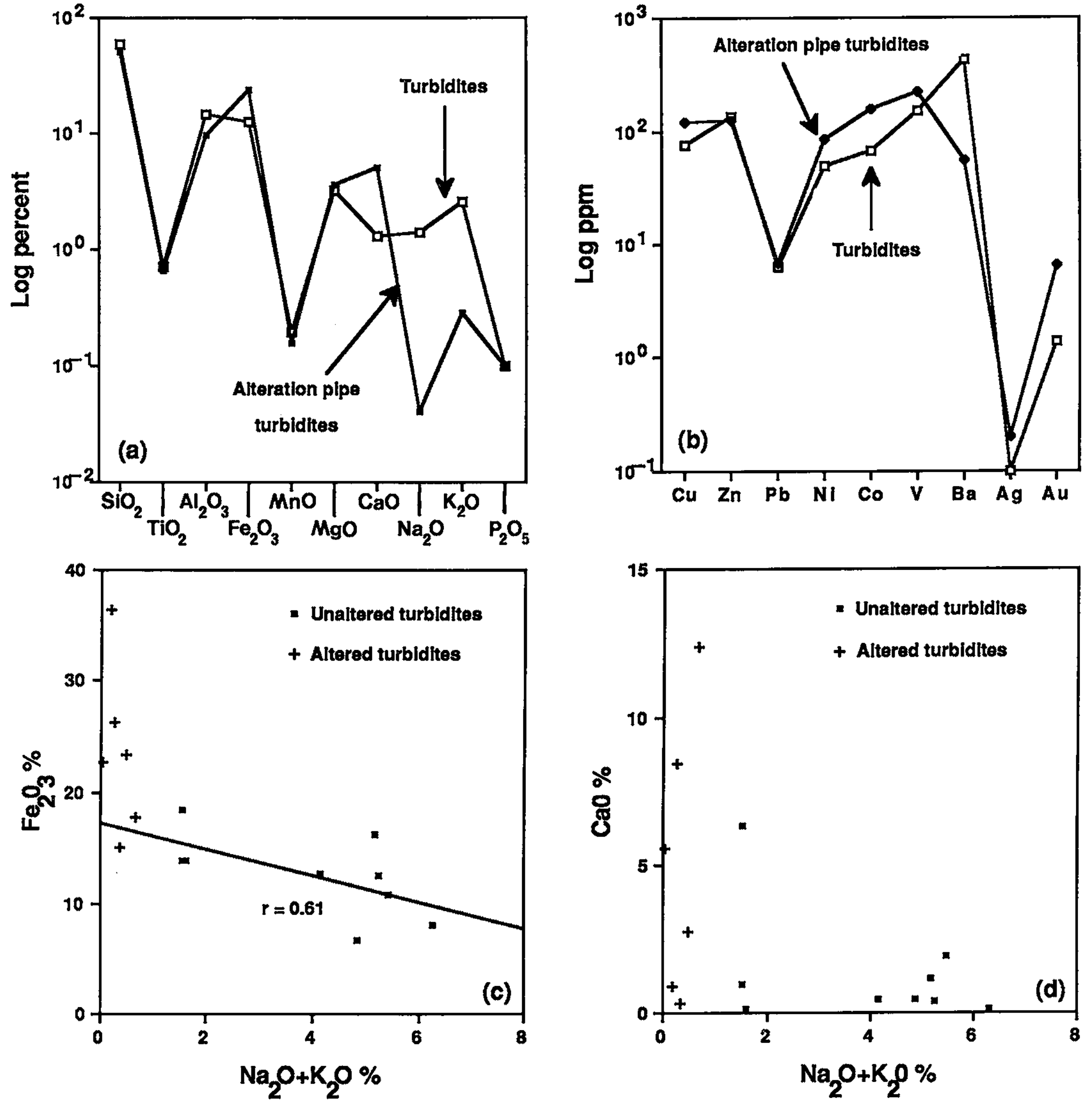

FIG. 8. Compositions of unaltered turbidites (host rock) and altered turbidites of the footwall alteration "pipe". (a): Average major-element composition; (b): average trace-element composition; (c): Fe_2O_3 *versus* alkalis; (d): CaO *versus* alkalis.

Zn–Cu-rich muds of the Atlantis II Deep, where they apparently result from seasonal variations in clastic input (Ross & Degens 1969), and in the Devonian Jason Pb–Zn deposit (Winn & Bailes 1987). The Soucy laminated sulfides also contain rare (≈ 1 cm) clastic turbidites; these are compositionally similar to the turbidites underlying the deposit and in the "banded" unit. Clastic turbidites have been reported from chemical sediments ranging from laminated sulfides at the Lower Proterozoic Sullivan Pb–Zn deposit (Hamilton *et al.* 1982), to Archean magnetite-rich iron-formation (Barrett & Fralick 1985).

The Soucy laminated sulfides bear a strong mesoscopic resemblance to the umbers associated with cupriferous massive sulfides of the Troodos ophiolite, Cyprus (Elderfield *et al.* 1972, Robertson & Hudson 1973). These classic ferromanganiferous oxide-rich umbers, which overlie volcanic-based massive sulfide deposits, consist mainly of goethite with subordinate quartz (Robertson 1976); fine clastic

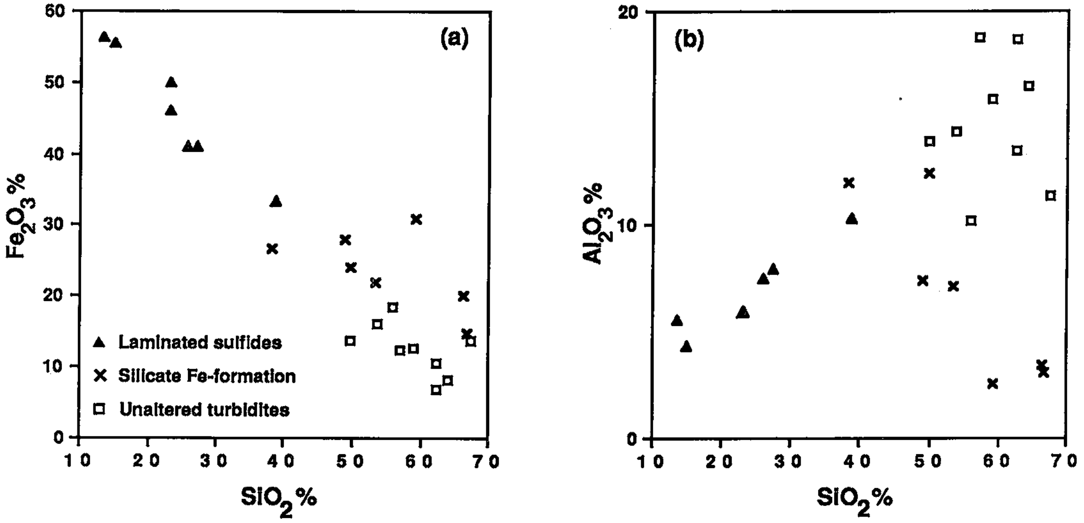

FIG. 9. Fe–Al–Si relationships among unaltered turbidites, laminated sulfides, and silicate iron-formation. (a): Fe_2O_3 *versus* SiO_2; (b): Al_2O_3 *versus* SiO_2.

laminations are also present. The umbers represent chemical precipitates formed by the interaction of metal-bearing hydrothermal solutions with oxygenated seawater. A similar origin has been ascribed to the chemical component of the Japanese hematite–chorite–quartz-bearing tetsusekiei which overlie the Kuroko ore deposits (Kalogeropoulos & Scott 1983). The tetsusekiei, which are <1 m thick, also contain an abundant clastic/tuffaceous component. In contrast, the very thick (up to 50 m) laminated sulfides at Soucy are dominated by pyrite–pyrrhotite, indicating that they were formed in contact with bottom waters which were anoxic, and contain quartzofeldspathic terrigenous rather than volcanic clastic material. Texturally, the closest modern analog is the sulfide-facies chemical sediment forming locally in the Atlantis II Deep, where various minerals precipitate within temperature- and salinity-stratified, oxygen-depleted layers, and settle on the basin floor as fine-grained laminated sediments (Ross & Degens 1969, Bäcker & Richter 1973, Bäcker 1976, Shanks & Bischoff 1977, Pottorf & Barnes 1983). Requisite to the formation and preservation of such lamination is the existence of a topographic sub-basin within which bottom-water circulation is limited or absent. Although the depositional setting at Soucy was likely a deeply foundered continental margin, rather than young ocean floor as in the Red Sea, topographically restricted euxinic sub-basins can form in the former setting, as evidenced by the mid-slope Orca Basin at 2000 m depth in the Gulf of Mexico (Shokes *et al.* 1977, Trabant & Presley 1978). We do not imply in the case of the inferred Soucy sub-basin that the bottom waters were hypersaline (as in the Red Sea and Orca Basin), but only that they were stagnant and euxinic.

Hydrothermal history

From the overall stratigraphic setting, we infer that the Soucy sub-basin was located on a foundered, deep-water continental margin block assumed to have been bounded by major faults. The presence of distal turbidite and pelitic interturbidite host sediments around the ore lens, and the abundance of thick gabbro sills, suggest a setting analogous to the early phase of spreading at the sediment-buried axis of the Gulf of California (Einsele 1982, 1985). One difference, however, is that hydrothermal solutions at Soucy apparently entered an anoxic bottom layer within a sub-basin, whereas in the Guaymas basin they are discharging into circulating oceanic bottom waters. We suggest that some of the sills at Soucy are synsedimentary, although most are coeval with the overlying Hellancourt basalts (Wares *et al.* 1988). The hydrothermal circulation system responsible for the massive sulfide deposit is inferred to have been driven by a heat source related to rising asthenosphere during early rifting. More advanced stages of rifting eventually led to pervasive sill intrusion on the foundered margin, and extrusion of basalt oceanward of the Soucy site.

A schematic outline of our model for the evolution of the hydrothermal systems which formed the massive and laminated sulfides of the Soucy deposit is given in Figure 10. Development can be envisaged in four main but overlapping stages.

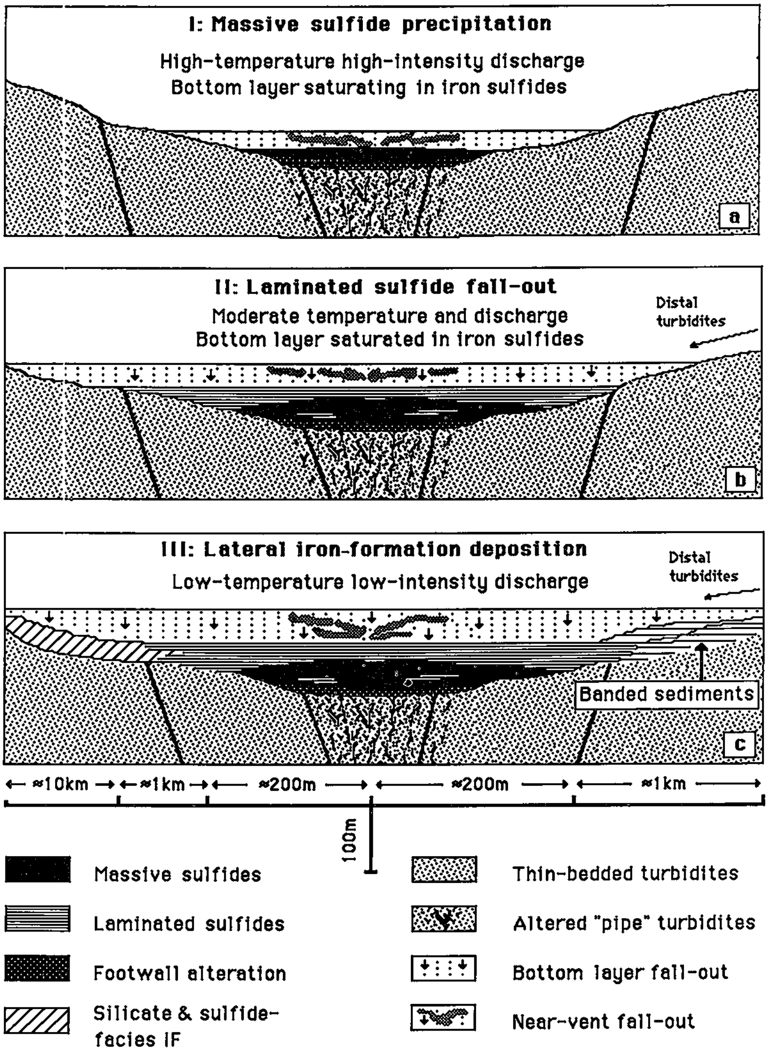

FIG. 10. Schematic model of two-stage hydrothermal activity at the Soucy deposit. A fault-bounded depression contains a relatively stagnant bottom-water layer which, once established, does not mix with overlying seawater. (a) An initial stage of intense, high-temperature hydrothermal discharge through poorly consolidated sediment forms a massive lens of Zn–Cu-bearing iron sulfides on the seafloor. Some iron is not precipitated but diffuses into the bottom-water layer. (b) Later, lower intensity discharge continues to supply iron to the bottom-water layer; when this layer becomes saturated, fine-grained iron sulfides rain down to produce the laminated sulfides. Minor Cu and Zn enrichment is present in laminated sulfides near the ore lens. (c) Low-intensity, low-temperature discharge continues, so that the bottom-water layer maintains saturation. This layer periodically overflows the sub-basin, carrying dissolved or finely particulate iron laterally. Overflow may become the dominant process as the sub-basin is gradually filled with laminated sulfides, leading to the formation of silicate- and sulfide-facies iron-formation peripheral to the sub-basin.

Stage 1. The central part of the Soucy sub-basin was fed directly from below by hydrothermal solutions, as indicated by the immediate footwall alteration and the veined feeder zone. The unusual curving nature of the veins indicates the sediments were not strongly lithified and did not fracture at the time they were traversed by the solutions. Discharging solutions in part simply may have diffused through the alteration zone; in the process, they strongly altered the sediment through removal of alkalis, Si and Al, and addition of Fe, Ca, and to a degree, trace metals.

Alkalies were re-precipitated in the immediate footwall, perhaps as a result of a pH decrease related to mixing with seawater. The lack of veins in this thin footwall zone may mean that these sediments, originally within a few meters of the sediment–seawater interface, were too unconsolidated to support a vein system. If so, a series of discharge points on the seafloor may have existed, such that the lateral extent of the massive sulfides is similar to that of the highly altered sediments. On the other hand, baked surficial metalliferous sediments supporting vein systems are known to occur in the Red Sea (Zierenberg & Shanks 1983). If such veins were present in the thin zone of immediate footwall alteration at Soucy, they were subsequently destroyed by further alteration.

Stage 2. An initial phase of high-temperature, intense discharge produced the massive Zn–Cu-rich sulfides of the ore lens near a vent or series of vents. Factor analysis suggests that Pb, Ag and Au were deposited with Cu–Zn sulfides, whereas Co and Au accompanied iron sulfide deposition. As we have not observed evidence for the existence of chimney-type structures, we suggest that thin wedges of massive sulfide formed, extending perhaps several meters laterally from individual discharge sites. With time, such wedges may have coalesced laterally and vertically to produce a massive sulfide lens, particularly if discharge points shifted within a restricted lateral area situated above the main fault-controlled zones of hydrothermal upwelling. Massive sulfide deposits of about the same size have been described from the Explorer Ridge and Mid-Atlantic Ridge by Tunnicliffe *et al.* (1986) and Rona *et al.* (1986), respectively. Although these latter deposits overlie basalts in an oxidized ocean-floor setting, they apparently formed as the result of numerous, migrating high-temperature discharge sites. Early generations of sulfides within seafloor deposits commonly have been recrystallized or partly replaced (or both) through "zone-refining" reactions with later hydrothermal solutions, as observed at Axial Seamount (Hékinian & Fouquet 1985, Hannington *et al.* 1986, Hannington & Scott 1988) and in the Galapagos axial valley (Embley *et al.* 1988). This may explain why the Soucy massive sulfides are more recrystallized and coarser than the overlying laminated sulfides, which, as discussed below, appear to represent bottom-layer fallout at much lower temperatures.

Stage 3. The Zn–Cu-rich sulfide precipitation phase was followed by a less intense, lower temperature phase which continued to inject hydrothermal solutions into a bottom-water layer. Iron sulfides were precipitated from this layer and were deposited together with thin, fine-grained clastic layers, producing the finely laminated texture. The occurrence of cm-scale wedges of laminated sulfides in the massive sulfide lens suggests that Fe-sulfide saturation of the bottom layer was achieved before the end of massive sulfide deposition. The presence of up to 50 m of laminated sulfides supports the long-term existence of a stable bottom-water layer. Based on the lateral extent of this lithology, the width of the sub-basin was ≈ 1 km. The laminated sulfides have an iron content comparable to that of the massive sulfides, but contain only ≈0.3% Zn and ≈0.2% Cu. The low base metal content of the Soucy laminated sulfides relative to those in the Red Sea may reflect the existence of a low-salinity bottom layer which was not capable of transporting metals laterally (as chloride complexes) to the same degree as the hypersaline Red Sea brines. Interestingly, the base metal composition of the Soucy laminated sulfides is similar to that of the Red Sea oxide-facies metalliferous sediments which represent more vent-distal facies (Bäcker 1976).

In the laminated sulfides, the size range of the pyrite particles, which we interpret as primary chemical precipitates, is comparable to the size of particles in hydrothermal smoke at active vents in open-ocean rift settings (Converse *et al.* 1984). It is therefore also possible that some of the pyrite particles represent smoke derived from nearby vents, but trapped in the non-circulating bottom layer. This process conceivably could operate in addition to precipitation from a supersaturated water layer. If some of the pyrite represents smoke particles, it differs from particles at modern vents, which are dominated by pyrrhotite with lesser amounts of sphalerite and chalcopyrite, though pyrite is not uncommon (Converse *et al.* 1984, Feely *et al.* 1987). The higher Cu–Zn–Pb–Ag–Au contents of the proximal relative to distal laminated sulfides reflect either a primary dispersion as initial precipitates, or the presence of redeposited fine-grained sulfides eroded from the vent area. Only a small proportion of smoke particles enriched in base and precious metals would have to mix with the ambient fallout of iron sulfides from the saturated bottom layer to produce the observed distribution. Enrichments in Cu and Zn in suspended matter near the inferred vent sites in the Atlantis II Deep bottom layer have been observed and are thought to occur as sulfides (Hartmann 1973).

Stage 4. The bottom-water layer periodically overflowed the edges of the sub-basin, carrying dissolved or finely particulate iron laterally. As the sub-basin gradually was filled with laminated sulfides, overflow of Fe-rich solutions may have become the dominant process. Overflow could have been instrumental in producing the silicate- and sulfide-facies iron-formations which are at least partly the lateral equivalents of the laminated sulfide unit (see also Gross 1983). Depending on the degree to which an iron-bearing bottom layer replaced more normal bottom waters, and the extent of contemporaneous turbidite sedimentation, three end-member types of lithological unit can be postulated: i) sulfide-facies iron-formation in reduced bottom waters with limited hemipelagic contribution; ii) silicate-facies iron-formation (containing ferrous and ferric iron) in less reduced bottom waters with a modest clastic contribution; and iii) "banded" sediments containing sulfide and clastic layers in reduced bottom waters with a significant input of turbidites. Because bottom topography was probably irregular, localized bottom-water layers separated by areas of variable turbidite deposition would have been the norm, leading to complex lateral and vertical facies relationships among these lithologies. Given that ocean waters in the Lower Proterozoic were probably more reduced than modern oceans (Maisonneuve 1982, Walker & Brimblecombe 1985), they may have provided some of the reduced sulfur in the sulfide-facies iron-formation (Fig. 10c). SIF may have formed authigenically and/or through metamorphic combination of iron and the fine-grained detrital quartz. Figure 10c schematically illustrates chemical sediments with a minor clastic component on one side of the Soucy sub-basin, and clastic/chemical sedimentation on the other (note the difference in lateral scales). In this model, the "banded" sediments, as well as the silicate- and sulfide-facies iron-formation, can also transgress over the laminated sulfides during waning stages of hydrothermal activity.

CONCLUSIONS

The Soucy massive sulfide deposit apparently formed in a sub-basin on the collapsed continental margin of a Lower Proterozoic rift system, prior to extrusion of basaltic seafloor. We infer that hydrothermal discharge was focused by faults related to the overall extensional regime. A massive sulfide lens, up to 40 m thick and 400 m in lateral extent, averaging $\approx$2% each of Cu and Zn, is conformably overlain by up to 50 m of laminated, very fine-grained sulfides containing only $\approx$0.3% Zn and $\approx$0.2% Cu. Laminated sulfides also extend laterally a few hundred meters beyond the massive sulfides; primary dispersion patterns are shown by Cu, Zn, Pb, Ag and Au, with highest values near the ore lens.

These relationships suggest that two different hydrothermal systems operated during sulfide deposition. The first was a high-intensity high-temperature stage that locally precipitated Cu–Zn-rich sulfides of the main ore lens. The second was a lower temperature, lower intensity stage which led to "fallout" of Fe-rich sulfides from a non-circulating bottom layer; thin clastic layers produce a finely laminated texture to these sulfides. The sharp boundary between the massive and laminated sulfides indicates that the intensity of hydrothermal discharge decreased abruptly. During deposition of the Fe-rich laminated sulfides, a base and precious metal-rich component was superimposed in the proximity of the ore lens. This component may reflect either a primary dispersion as initial precipitates, or the presence of redeposited fine-grained sulfides eroded from the vent area. The chemical component of interbedded silicate- and sulfide-facies iron-formation and interlayered sulfide/clastic sediments occurring along strike from the laminated sulfides is interpreted to have resulted from spillover effects from the hydrothermally influenced bottom-water layer in the sub-basin.

The Soucy deposit shares some general features with Besshi-type deposits, but also records stratigraphic, sedimentological, and hydrothermal characteristics which have not been recognized. This is partly a result of the low degree of metamorphism in the foreland belt of the Labrador Trough, relative to amphibolite-grade terranes of classic Besshi-type deposits.

ACKNOWLEDGEMENTS

We thank the Ministère de L'Énergie et des Ressources du Québec (MERQ) for permission to publish this paper. We thank Dr. S.D. Scott and an anonymous reviewer for their constructive comments on the paper, and Dr. W. MacLean for reviewing an earlier version of the manuscript. Mr. Tom Bensics did much of the drafting. This work was supported through of a research contract from the MERQ on the metallogeny of the northern Labrador Trough.

REFERENCES

BARRETT, T.J. & FRALICK, P. (1985): Sediment redeposition in Archean iron formation: examples from the Beardmore–Geraldton Greenstone Belt, Ontario. *J. Sed. Petrology* **55**, 205-212.

BÄCKER, H. (1976): Facies und chemische Zusammensetzung rezenter Ausfällungen aus Mineralquellen in Roten Meer. *Geol. Jahrb.* **17**, 151-172.

______ & RICHTER, H. (1973): Die rezente hydrothermal-sedimentäre Lagerstätte Atlantic-II Tief im Roten Meer. *Geol. Rundschau* **62**, 697-741.

BIGNELL, R.D., CRONAN, D.S. & TOOMS, J.S. (1976): Red Sea brine metalliferous precipitates. *Geol. Assoc. Can. Spec. Pap.* **14**, 147-179.

CLARK, T. (1987): Stratigraphie, pétrographie et pétrochimie de la Formation de Fer de Baby, région du lac Hérodier, Fosse du Labrador. *Min. de L'Énergie Res. Qué.* **ET-87-13**.

CONVERSE, D.R., HOLLAND, H.D. & EDMOND, J.M. (1984): Flow rates in the axial hot springs of the East Pacific Rise (21°N): implications for heat budget and the formation of massive sulphide deposits. *Earth Planet. Sci. Lett.* **69**, 159-175.

DIMROTH, E. (1972): The Labrador Geosyncline revisited. *Amer. J. Sci.* **272**, 487-506.

______ (1981): Labrador Geosyncline: type example of early Proterozoic cratonic reactivation. *In* Precambrian Plate Tectonics (A. Kroner, ed.). *Developments in Precambrian Geology* **4**, 331-352. Elsevier, Amsterdam.

______ & DRESSLER, B. (1978): Metamorphism of the Labrador Trough. *In* Metamorphism in the Canadian Shield (J.A. Fraser & W.W. Heywood, eds.). *Geol. Surv. Can. Rep.* **78-10**, 215-236.

DOI, M. (1961): The historical review of the genesis of the Besshi ore deposits. *Mining Geol.* **11**, 151-156.

EINSELE, G. (1982): Mechanism of sill intrusion into soft sediment and expulsion of pore water. *In* Initial Reports of Deep Sea Drilling Project **64**(2), 1169-1176. U.S. Gov. Printing Office, Washington, DC.

______ (1985): Basaltic-sill–sediment complexes in young spreading centers: Genesis and significance. *Geology* **13**, 249-252.

ELDERFIELD, H., GASS, I.G., HAMMOND, A. & BEAR, L.M. (1972): The origin of ferromanganese sediments associated with the Troodos massif of Cyprus. *Sedimentology* **19**, 1-19.

EMBLEY, R.W., JONASSON, I.R., PERFIT, M.R., FRANKLIN, J.M., TIVEY, M.A., MALAHOFF, A., SMITH, M.S. & FRANCIS, T.S.G. (1988): Submersible investigations of an extinct hydrothermal system on the Galapagos Ridge: sulfide mounds, stockwork zone and differentiated lavas. *Can. Mineral.* **26**, 517-539.

FEELY, R.A., LEWISON, M., MASSOTH, G.J., ROBERT-BALDO, G., LAVELLE, J.W., BYRNE, R.H., VON DAMM, K.L. & CURL, H.C., JR. (1987): Composition and dissolution of black smoker particulates from active vents on the Juan de Fuca Ridge. *J. Geophys. Res.* **92**, 11347-11363.

FEISS, P.G. & HAUCK, S.A. (1980): Tectonic setting of massive sulphide deposits in the southern Appalachians. *In* Proceedings of the Fifth Quadrennial IAGOD Symposium. Schweitzerbart'sche Verlag, 567-580.

FOX, J.S. (1984): Besshi-type volcanogenic sulphide deposits - a review. *Can. Inst. Mining Metall. Bull.* **77**, 57-68.

______, FARQUHAR, R., RUI, I. & COOK, N. (1988): Genesis of basalt-hosted massive sulphide deposits from the Trondheim and Sulitjema districts, Norway: ore lead isotopic considerations. *Mineral. Deposita* (in press).

FRALICK, P.W., BARRETT, T.J. & SCHNIEDERS, B.R. (accepted): Sulfide-facies iron-formation and pyritic structures at the Archean Morley occurrences, northern Ontario. *Can. Mineral.*

FRANKLIN, J.M., LYDON, J.W. & SANGSTER, D.F. (1981): Volcanic-associated massive sulfide deposits. *Econ. Geol. 75th Ann. Vol.*, 485-627.

FRYER, B.J. (1972): Age determinations in the Circum-Ungava geosyncline and the evolution of Precambrian iron formations. *Can. J. Earth Sci.* **9**, 652-663.

FRIETSCH, R., PAPUNEN, H. & VOKES, F.M. (1979): The ore deposits of Finland, Norway, and Sweden - A review. *Econ. Geol.* **74**, 975-1001.

GEE, D.G. (1975): A tectonic model for the central part of the Scandinavian Caledonides. *Amer. J. Sci.* **275A**, 468-515.

GRAHAM, U.M., BLUTH, G.J. & OHMOTO, H. (1988): Sulfide–sulfate chimneys on the East Pacific Rise, 11° and 13°N latitudes. Part I: mineralogy and paragenesis. *Can. Mineral.* **26**, 487-504.

GROSS, G.A. (1983): Tectonic systems and the deposition of iron-formation. *Precambrian Res.* **20**, 171-187.

GUSTAFSON, L.B. & WILLIAMS, N. (1981): Sediment-hosted stratiform deposits of copper, lead, and zinc. *Econ. Geol. 75th Ann. Vol.*, 139-178.

HAMILTON, J.M., BISHOP, D.T., MORRIS, H.C. & OWENS, O.E. (1982): Geology of the Sullivan orebody, Kimberley, B.C., Canada. *In* Precambrian Massive Sulphide Deposits (R.W. Hutchinson, C.D. Spence & J.M. Franklin, eds.). *Geol. Assoc. Can. Spec. Pap.* **25**, 597–665.

HANNINGTON, M. & SCOTT, S.D. (1988): Mineralogy and geochemistry of a hydrothermal silica–sulfide–sulfate spire in the caldera of Axial Seamount, Juan de Fuca Ridge, *Can. Mineral.* **26**, 603-625.

______, PETER, J.M. & SCOTT, S.D. (1986): Gold in sea-floor polymetallic deposits. *Econ. Geol.* **81**, 1867-1883.

HARTMANN, M. (1973): Untersuchungen von suspendierten Material in den Hydrothermallaugen des Atlantis-II-Tiefes. *Geol. Rundschau* **62**, 742-754.

HÉKINIAN, R. & FOUQUET, Y. (1985): Volcanism and metallogenesis of axial and off-axial structures on the East Pacific Rise near 13°N. *Econ. Geol.* **80**, 221-249.

HOFFMAN, P.F. (1987): Early Proterozoic foredeeps, foredeep magmatism and Superior-type iron formations of the Canadian Shield. *In* Proterozoic Lithospheric Evolution (A. Kröner, ed.). *Amer. Geophys. Union, Geodyn. Ser.* **17**, 85-98.

HYNES, A. (1978): Early recumbent folds in the northeastern part of the northern Labrador trough. *Can. J. Earth Sci.* **15**, 245-252.

JAMES, H.L. (1954): Sedimentary facies of iron-formation. *Econ. Geol.* **49**, 235-285.

KANEHIRA, K. & TATSUMI, T. (1970): Bedded cupriferous iron sulfide deposits in Japan, a review. *In* Volcanism and Ore Genesis (T. Tatsumi, ed.). Tokyo Univ. Press, Tokyo, 51-76.

KLEIN, C., JR. (1979): Changes in mineral assemblages with metamorphism of some banded Precambrian iron-formations. *Econ. Geol.* **68**, 1075-1088.

KALOGEROPOULOS, S.I. & SCOTT, S.D. (1983): Mineralogy and geochemistry of tuffaceous exhalites (tetsusekiei) of the Fukazawa Mine, Hokuroku District, Japan. *Econ. Geol. Monogr.* **5**, 412-432.

KLAU, W. & LARGE, D.E. (1980): Submarine exhalative Cu–Pb–Zn deposits, a discussion of their classification and metallogenesis. *Geol. Jahrb., sec. D, no. 40*, 13-58.

KOSKI, R.A., CLAGUE, D.A. & OUDIN, E. (1984): Mineralogy and chemistry of massive sulfide deposits from the Juan de Fuca Ridge. *Geol. Soc. Amer. Bull.* **95**, 930-945.

LEGALLAIS, C.J. & LAVOIE, S. (1982): Basin evolution of the lower Proterozoic Kaniapiskau Supergroup, central Labrador miogeocline (trough), Quebec. *Bull. Can. Petroleum Geol.* **30**, 150-166.

Maisonneuve, J. (1982): The composition of the Precambrian ocean waters. *Sediment. Geol.* **31**, 1-11.

Mattinen, P.R. & Bennett, G.H. (1986): The Green Mountain massive sulphide deposit. Besshi-style mineralization within the California Foothills copper-zinc belt. *J. Geochem. Expl.* **25**, 185-200.

Nilsen, O. (1978): Caledonian sulphide deposits and minor iron-formations from the southern Trondheim region, Norway. *Norges Geol. Unders., no.* **340**, 35-85.

Pottorf, R.J. & Barnes, H.L. (1983): Mineralogy, geochemistry, and ore genesis of hydrothermal sediments from the Atlantis II Deep, Red Sea. *Econ. Geol. Monogr.* **5**, 198-223.

Robertson, A.H.F. (1976): Origins of ochres and umbers: Evidence from Skouriotissa, Troodos massif, Cyprus. *Inst. Mining Metall. Trans.* **85(B)**, 245-251.

——— & Hudson, J.D. (1973): Cyprus umbers: chemical precipitates on a Tethyan ocean ridge. *Earth Planet. Sci. Lett.* **28**, 285-294.

Rona, D.A., Klinkhammer, G., Nelsen, T.A., Trefry, J.H. & Elderfield, H. (1986): Black smokers, massive sulphides and vent biota at the Mid-Atlantic Ridge. *Nature* **321**, 33-37.

Ross, D.A. & Degens, E.T. (1969): Shipboard collection and preservation of sediment samples collected during Chain 61 from the Red Sea. *In* Hot Brine and Recent Heavy Metal Deposits in the Red Sea (E.T. Degens & D.A. Ross, eds.), 363-367. Springer-Verlag, N.Y.

Sauvé, P. & Bergeron, R. (1965): Région des lacs Gérido et Thévenet. *Min. Richesses Naturelles du Québec, rapport géol.* **104.**

Shanks,, W.C., III & Bischoff, J.L. (1977): Ore transport and deposition in the Red Sea goethermal system: a geochemical model. *Geochim. Cosmochim. Acta* **41** 1507-1519.

Shokes, R.F., Trabant, P.K., Presley, B.J. & Reid, D.F. (1977): Anoxic, hypersaline basin in the northern Gulf of Mexico. *Science* **196**, 1443-1446.

Stephens, M.B., Swinden, H.S. & Slack, J.F. (1984): Correlation of massive sulfide deposits in the Appalachian-Caledonian orogen on the basis of paleotectonic setting. *Econ. Geol.* **79**, 1442-1478.

Stockwell, C.H. (1982): Proposals for the time-classification and correlation of Precambrian rocks and events in Canada and adjacent areas of the Canadian Shield. *Geol. Surv. Can. Pap.* **82-19**, Part I.

Trabant, P.K. & Presley, B.J. (1978): Orca Basin, anoxic pool on the continental slope, northwest Gulf of Mexico. *In* Framework, Facies and Oil-Trapping Characteristics of the Upper Continental Margin (J.M. Coleman, ed.). *Amer. Assoc. Petroleum Geol., Stud. Geol.* **7**, 303-311.

Tunnicliffe, V., Botros, M, de Burgh, M.E., Dinet, A., Johnson, H.P., Juniper, S.K. & McDuff, R.E. (1986): Hydrothermal vents of Explorer Ridge, northeast Pacific. *Deep-Sea Res.* **33**, 401-412.

Walker, J.C.G. & Brimblecombe, P. (1985): Iron and sulfur in the pre-biologic ocean. *Precambrian Res.* **28**, 205-222.

Wardle, R.J. & Bailey, D.G. (1981): Early Proterozoic sequences in Labrador. *In* Proterozoic Basins in Canada (F.H.A. Campbell, ed.). *Geol. Surv. Can. Rep.* **81-10.**

Wares, R.P., Berger, J. & St.-Seymour, K. (1988): Synthèse métallogénique des indices de sulfures au nord du 57°ème parallèle, Fosse du Labrador. *Mineral. Richesses Naturelles du Québec,* **MB-88-05.**

Winn, R.D., Jr. & Bailes, R.J. (1987): Stratiform lead-zinc sulfides, mudflows, turbidites: Devonian sedimentation along a submarine fault scarp of extensional origin, Jason deposit, Yukon Territory, Canada. *Bull. Geol. Soc. Amer.* **98**, 528-539.

Zierenberg, R.A. & Shanks, W.C., III (1983): Mineralogy and geochemistry of epigenetic features in metalliferous sediment, Atlantis II Deep, Red Sea. *Econ. Geol.* **78**, 57-72.

Received October 22, 1987; revised manuscript accepted May 28, 1988.